Available online at www.sciencedirect.com

ScienceDirect

Proceedings of the Combustion Institute 37 (2019) 5697–5704

Proceedings of the Combustion Institute

www.elsevier.com/locate/proci

Modulation of heat transfer for extended flame stabilization in porous media burners via topology gradation

Sadaf Sobhani*, Danyal Mohaddes, Emeric Boigne, Priyanka Muhunthan, Matthias Ihme

Department of Mechanical Engineering, Stanford University, Stanford, CA 94305, United States

Received 30 November 2017; accepted 28 May 2018
Available online 25 June 2018

Abstract

Porous media burners (PMBs) enable enhanced combustion performance by internally recirculating heat released from the combustion products upstream to the reactants via an inert solid matrix. Compared to conventional free-flame systems, PMBs are characterized by higher burning velocities, extended flammability, and lower emissions of NO_x. Current PMB implementations utilize a two-zone concept in which the flame stabilizes at the interface between two porous matrices of different topologies. In this work, a PMB design having a spatially graded porous matrix is proposed, supported by theoretical analysis of the governing equations and constitutive relations. Through computations and experiments, it is shown that the proposed physical design of the porous matrix results in a significant enhancement of the power-dynamic range and in excess of 50% higher blow-off limits compared to current designs. This is achieved through gradation in topology (i.e. porosity, pore diameter, cell diameter, etc.), which enables a continuous variation of radiative extinction properties as well as interphase heat exchange, allowing the flame to stabilize dynamically within the porous matrix and for a wider range of operating conditions.

Keywords: Porous media combustion; Ceramic foams; Heterogeneous combustion; Flame stabilization; Premixed combustion

1. Introduction

Lean premixed combustion mitigates emissions and efficiency concerns related to incomplete mixing of fuel and air, but can also lead to undesirable phenomena such as flashback and blow-off. Proper flame stabilization is a critical safety and reliability concern, which highlights the need for innovative combustor concepts. Porous media burners (PMBs) facilitate excess enthalpy combustion, the process of exchanging enthalpy from the combustion products to the incoming reactants, which enables higher burning velocities and extended lean flammability limits [1]. Additionally, the high heat capacity and conductivity of the solid matrix

* Corresponding author.
E-mail address: ssobhani@stanford.edu (S. Sobhani).

https://doi.org/10.1016/j.proci.2018.05.155
1540-7489

stabilize fluctuations in thermal load and fuel/air ratio, thereby mitigating the propensity for blow-off and other combustion instabilities. Several models and burner designs have been previously proposed that aim to culminate the effects of the solid phase thermal properties, internal heat recirculation and interphase heat exchange to further the operational range extension [2].

In a PMB, the burning velocity can exceed that of an unstrained laminar flame due to the greater thermal conductivity and radiation within the solid phase as compared to that of the gas phase. Although the porous matrix extends the flame stability, the resulting coupling of the chemical energy release in the gas phase and conjugate heat transfer with the solid phase makes characterizing the flame behavior in PMBs a particularly challenging problem. Buckmaster and Takeno [3] proposed a thermal model to predict the flame stabilization in PMBs, stating that during steady-state operation, the flame is positioned in a region where the flame speed is positively correlated with the axial location of the flame. PMB designs based on these thermal models reported approximately a 3:1 range of firing capacities, referred to as turndown ratio or power-dynamic range, for embedded flames [4].

As an alternative to balancing effective flame speeds to achieve flame stabilization, Trimis and Durst [5] proposed a quenching technique that anchors the flame at a fixed position. This design is based on the concept of a critical Péclet number. The flame is stabilized at the interface of the sub- and super-critical regions, and is therefore referred to as a two-zone interface-stabilized — or step — PMB. A power-dynamic range up to 20:1 was reported for this design [5].

The quenching technique of the step PMB is based on the notion that the upstream region serves as a flashback arrester. Barra et al. [6] found that larger upstream pores and lower thermal conductivity help prevent flashback by limiting heat exchange from the solid. Sufficient flashback prevention in this design implies a performance trade-off, since limiting the reactant mixture preheating hinders the extension of both the lean flammability and blow-off limits in the burner. To address this limitation, an alternative stabilization technique was proposed by Voss et al. [7] based on a spatially varying cross-sectional area of the burner. Contrary to the fixed-flame location of the step burner, in this technique the flame stabilizes at a location where the Darcy velocity balances the flame speed inside the porous matrix. Experimental studies have successfully implemented this design at high burning velocities for syngas [7] and methane [8] with a reported power-dynamic range of approximately 6:1. However, a large angle of divergence is required to achieve adequate deceleration of the flow for some applications, which may result in restrictively large cones, radial heat losses, and an inhomogeneous mean velocity profile due to the expanding flow.

The design proposed in this paper is based on a topology gradation of the porous matrix, which addresses the aforementioned challenges in PMB design: reliable operation of premixed flames, enhanced heat recirculation without flashback, and extended blow-off limit. Pore topology is commonly defined by pore diameter, cell diameter, porosity, and other parameters outlined in [9]. The structure of porous foams consists of rounded polyhedra (cell diameter) connected by openings or windows (pore diameter). The topology of the porous material directly impacts the local heat transfer, and thereby the flame behavior. The impact of porosity and pore diameter on the properties of the flame is examined theoretically in Section 2 by non-dimensionalizing the volume-averaged governing equations and isolating the constitutive relations that are strongly dependent on the pore topology. The newly proposed design, referred to as *graded PMB*, is studied numerically using a 1D volume-averaged model and experimentally using a series of Silicon Carbide (SiC) porous foams instrumented to measure the temperature profiles and pressure drop. The experimental investigation is presented in Section 3, comparing results to those of a *step PMB* to illustrate the performance advantages of the graded design, with power-dynamic ratios near 50:1 and less than 5.4% pressure drop. The paper closes by offering conclusions and discussing aspects of possible manufacturing techniques for continuously graded porous foams.

2. Theoretical and computational investigation

2.1. Theoretical analysis

The equations governing the combustion in porous media are derived by volume-averaging of the transport equations for a chemically reacting gaseous system [2]. Effects of conduction and radiation in the solid phase, and heat exchange between solid and gas are incorporated in the equations. The following assumptions are used in the current model formulation: (i) Dufour, Soret, and viscous dissipation effects are negligible, (ii) the burner is radiating to a black body at 300 K from the inlet and outlet, and itself acts as a gray body, (iii) gas phase radiation is negligible, (iv) the solid matrix is chemically inert and potential catalytic effects are neglected, (v) pressure drop is evaluated using the Darcy–Forchheimer equation with Ergun's relations [10], and (vi) the effect of turbulence is neglected since only subcritical Reynolds numbers are considered. With these assumptions, the governing equations for mass, species, and energy

conservation take the following form:

$$\partial_t(\rho_g\epsilon) + \partial_x(\epsilon\rho_g u) = 0, \tag{1a}$$

$$\epsilon\rho_g(\partial_t Y_i + u\partial_x Y_i) = -\partial_x(\epsilon\rho_g V_i Y_i) + \epsilon\dot{\omega}_i, \tag{1b}$$

$$\begin{aligned}\epsilon\rho_g c_g\big(\partial_t T_g + u\partial_x T_g\big) &= \partial_x\big(\lambda_g\partial_x(\epsilon T_g)\big)\\ &\quad - \rho_g\Big(\sum\nolimits_{i=1}^{N_s} c_{g,i}V_i Y_i\Big)\partial_x(\epsilon T_g)\\ &\quad - h_v(T_g - T_s) + \epsilon\dot{q}_H,\end{aligned} \tag{1c}$$

$$\begin{aligned}(1-\epsilon)\rho_s c_s\partial_t(T_s) &= \partial_x(\lambda_{s,\mathrm{eff}}\partial_x T_s) - \partial_x\dot{q}_R\\ &\quad + h_v\big(T_g - T_s\big),\end{aligned} \tag{1d}$$

where subscripts g and s correspond to the gas and solid phase, respectively, 'eff' refers to the effective transport property, ϵ is the porosity, and u is the average interstitial gas velocity. Conventional nomenclature is employed and further details can be found in [11].

The radiative source term, appearing in Eq. (1d) takes the form:

$$\partial_x\dot{q}_R = 2\kappa(1-\Omega)\big(2\sigma T_s^4 - \big[\dot{q}_R^+ + \dot{q}_R^-\big]\big), \tag{2}$$

where κ is the radiative heat extinction coefficient, Ω is the scattering albedo and σ is the Stefan–Boltzmann constant. The radiant heat fluxes in the forward (+) and backward (−) directions are expressed using the Schuster–Schwarzschild approximation [12]:

$$d_x\dot{q}_R^+ = -\kappa(2-\Omega)q_R^+ + \kappa\Omega q_R^- + 2\kappa(1-\Omega)\sigma T_s^4, \tag{3}$$

$$-d_x\dot{q}_R^- = -\kappa(2-\Omega)q_R^- + \kappa\Omega q_R^+ + 2\kappa(1-\Omega)\sigma T_s^4. \tag{4}$$

The pressure drop is evaluated using the Darcy–Forchheimer equation:

$$d_x P = -\frac{\mu}{K_1}u_D - \frac{\rho}{K_2}u_D^2, \tag{5}$$

where u_D is the Darcy velocity, K_1 is the intrinsic permeability and K_2 is the non-Darcian drag coefficient:

$$K_1 = \frac{d^2\epsilon^3}{150(1-\epsilon)^2}\ ,\ K_2 = \frac{d\epsilon^3}{1.75(1-\epsilon)}. \tag{6}$$

The radiative heat extinction coefficient was based on a geometric optics model, previously validated by Hsu and Howell [13], where $\kappa = 3(1-\epsilon)/d$. Patel and Talukdar [14] determined the radiative properties of a ceramic foam by solving the radiative transfer equations in a 3D cubic unit cell, reporting a positive correlation between pore density and extinction coefficient. Assuming that the pore diameter decreases with increasing pore density, this is consistent with the geometric optics model that predicts an increase in the extinction coefficient with decreasing pore diameter. Scattering albedo, however, was found to be unaffected by pore density [14]. Therefore the extinction coefficient and optical depth are increased with decreasing pore diameter. As such, if the porous media is sufficiently opaque, radiation becomes ineffective at recirculating heat.

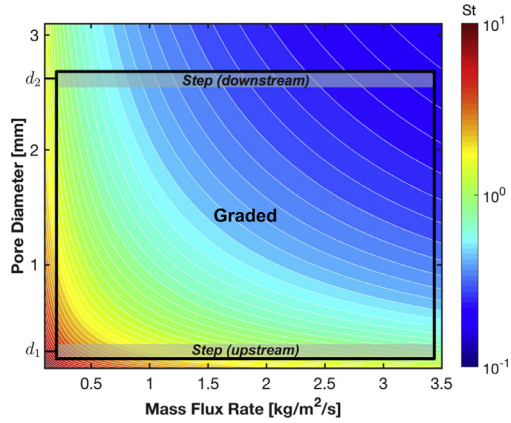

Fig. 1. Contour map of the local Stanton number as a function of pore diameter, d, and mass flux rate, $\dot{m}''$. Ranges of Stanton numbers accessed in the step burners versus the graded burners are illustrated.

After non-dimensionalization of Eq. (1c) with respect to reference quantities, the ratio of the convective transport to the interphase heat exchange terms in the gas-phase temperature equation results in the Stanton number, defined as

$$\mathrm{St} = \frac{\mathrm{Nu}}{\mathrm{Pe}},\ \text{with}\ \mathrm{Pe} = \frac{u_D}{a\alpha}\ \text{and}\ \mathrm{Nu} = \frac{h_v d}{a\lambda}, \tag{7}$$

where Pe is the Péclet number, Nu is the Nusselt number, α is the gas thermal diffusivity, a is the specific surface area, h_v is the volumetric heat transfer coefficient, and d is the pore diameter. Depending on its sign, the term $(T_g - T_s)$ can quantify a source or a sink in the temperature equation of the gas phase, Eq. (1c). Specifically, upstream of the flame, the solid, which is heated by solid-solid radiation and conduction, transfers heat to the incoming cold reactants (i.e. source term), whereas the hot combustion products transfer heat to the solid downstream of the flame (i.e. sink term). To model this heat exchange, an empirical correlation for the Nusselt number in ceramic foams is used: $\mathrm{Nu} = C\mathrm{Re}^m\mathrm{Pr}^n$, where the coefficients C, m, n equal 3.7, 0.38, and 0.25, respectively [15]. The Reynolds and Prandtl numbers are defined as: $\mathrm{Re} = \rho_g u_D d/\mu_g$, $\mathrm{Pr} = c_g\mu_g/\lambda_g$, respectively.

Effects of pore diameter, d, and mass flux rate, $\dot{m}''$, on the Stanton number are illustrated in Fig. 1, where the values for the thermal properties correspond to burnt gases. Figure 1 illustrates the

Table 1
Geometry of the burners, where x is the axial position, L is the burner length, x_I is the length of the upstream section, ϵ is porosity, and d is pore diameter; subscripts 1 and 2 denote values at the inlet and outlet, respectively, $\Delta d = d_2 - d_1$, $\Delta\epsilon = \epsilon_2 - \epsilon_1$, $\mathcal{H}(\xi)$ denotes the Heaviside function.

Burner	Interface (Step)	Continuous (Graded)
1	$\epsilon = (\epsilon_1 + \epsilon_2)/2$ $d(x) = d_1 + \Delta d\mathcal{H}(x - x_I)$	$\epsilon = (\epsilon_1 + \epsilon_2)/2$ $d(x) = d_1 + \Delta d(x/L)$
2	$\epsilon(x) = \epsilon_1 + \Delta\epsilon\mathcal{H}(x - x_I)$ $d(x) = d_1 + \Delta d\mathcal{H}(x - x_I)$	$\epsilon(x) = \epsilon_1 + \Delta\epsilon(x/L)$ $d(x) = d_1 + \Delta d(x/L)$

decrease of interphase heat exchange with increasing mass flux ($\mathrm{St} \propto (\dot{m}''d)^{m-1}$), which reduces preheating and eventually results in flame blow-off. As highlighted by the empirical correlations discussed, closure models for the 1D volume-averaged equations are parametrized by two main topological features, namely pore diameter and porosity, with the assumption that other features such as pore density and cell diameter can be deduced through a deterministic mapping.

Recognizing that the heat transfer between the solid and gas, quantified using the Stanton number, as well as the radiative heat transfer in the solid are primarily dependent on the local pore topology, a comparative study of flame stability and pressure drop between conventional step PMBs and those with graded matrix topologies was conducted. The porous matrix in graded PMBs can be designed to accommodate different heat outputs over a wider range of operating conditions without resorting to a flame quenching approach. In this study, gradation of the porous matrix was achieved by changing the local pore diameter, porosity, or both simultaneously. Two of the configurations examined for step and graded PMBs are shown in Table 1. Prompted by the analysis of the governing equations and constitutive relations for heat exchange and thermal radiation, the following numerical and experimental studies demonstrate and experimentally validate the impact of a graded porous matrix on the salient features of a PMB.

2.2. Computational method and setup

Numerical simulations were performed using the Cantera [16] 1D reacting flow solver, which was adapted to account for the coupling between the gas and solid phases. Detailed reaction chemistry for methane/air was modeled using the GRI 2.11-mechanism [17], which includes nitrogen chemistry. A steady-state solution is obtained using a Newton-minimization step to reduce the residuals. In case of poor convergence, the solver switches to a transient problem. More details of the computational method can be found in [11].

To facilitate comparisons, the length, material, and pore densities modeled correspond to those of the experimental study, described in Section 3. The total length of all burners considered is $L =$ 7.62 cm, and the length of the upstream section, serving as a flashback arrestor for the interface-stabilized burner is $x_I = L/2$. A graded topology burner of the same total length was constructed with the same porosity and pore-diameter limits, but with either a linearly varying or a constant profile (see Table 1).

The effective thermal conductivity, $\lambda_{s,\,\mathrm{eff}}$, in the porous solid is determined by the material microstructure and the conductivity of its constituents using PuMA [18]. For this, a 25 μm resolution tomographic reconstruction of the 10 ppi (pores per inch) SiC foam used in the experimental investigation is imported to PuMA. The steady state heat conduction equation is then solved using a finite difference method with a prescribed temperature differential in the simulation direction and periodic boundary conditions in the side directions. This process is repeated for the all three directions. An effective thermal conductivity is found to be isotropic and equal to 8.7 W/mK, which is approximated as a constant, thereby neglecting the weak dependence on the local topology for the conditions considered in the present work [13]. All simulations and experiments in the current work are done using the same material (i.e. SiC).

Using this simulation technique, a parametric study exploring inlet mass flux rate and equivalence ratio was carried out to compare the stability range, pressure drop and emissions of the newly proposed graded topology burner against the conventional step burner. Starting with a stable operating point, simulations were performed by incrementally increasing or reducing the mass flux rate until flame blow-off or flashback, respectively. Predicted mass flux rates above the validity of the closure models used for interphase heat transfer were discarded. Results from this analysis are discussed next.

2.3. Parametric analysis

Flame stability, pressure drop, and NO_x emissions of step and graded topology PMBs were investigated computationally. For burner 1, both designs had a constant porosity $\epsilon = 0.8$ and increasing nominal pore diameters (i.e. d=1/ppi), $d_1 = 0.39$ mm and $d_2 = 2.54$ mm, corresponding to 65 ppi and 10 ppi foams, respectively. For burner 2, the pore diameter profile was the same as burner 1, but the porosity was graded from $\epsilon_1 = 0.75$ to $\epsilon_2 = 0.85$. The stability envelopes for both burn-

ers are shown in Fig. 2 for equivalence ratios 0.55 to 0.65 since at higher equivalence ratios, the predicted mass flux rates were outside of the valid range of the closure models used for interphase heat transfer. Trends in flame stability at these lean conditions confirm the predictions of the theoretical analysis and motivated further experimental investigations.

Figure 2a,b illustrate the stability envelopes of burner 1, corresponding to step and graded PMBs, shown with isocontours of pressure drop, mass flux rate associated with laminar flame speed indicated by S_L, together with measurements at the experimentally determined maximum mass flux rates (further described in Section 3.3). As predicted by the analysis of the optical depth and interphase heat exchange in the governing equations, a graded PMB expands the range of stable operating conditions compared to that of a step PMB. Graded burner 1 reached approximately 75% higher blow-off mass flux rates than the step PMB, while maintaining similar NO_x emissions (not shown). Figure 2c,d illustrate the stability envelopes of burner 2. The pressure drop is generally lower for this burner, although the increase in flame stability is less pronounced. In the burners with a step profile in pore topology, the flame primarily stabilizes slightly downstream of the interface, where the pore diameter is larger. However, in the graded burner, the flame is not anchored to any specific location but rather is dynamically stabilized, resulting in the following practical consequences: (1) First, this feature is relevant to the pressure drop, which is inversely proportional to the pore diameter and directly proportional to the viscosity [10]. Viscosity at the flame is significantly increased, but its effect on pressure drop is mitigated if the flame is stabilized within larger pores, as in the step burner. Therefore, the step PMB is predicted to have lower pressure drop. (2) Second, the interface- versus continuous-flame stabilization affects the axial Stanton number profile and consequently the heat transfer properties, as illustrated in Fig. 3.

Temperature profiles, which confirm the excess enthalpy behavior in PMBs, are shown in Fig. 3a. The continuous-flame stabilization of the graded PMB is compared to the anchored flames of the step PMB, corresponding to the stability map of burner 1 at $\phi = 0.55$ (see Fig. 2). In Fig. 3b, the coordinate system has been centered at the flame location to examine trends in the local Stanton number. At higher mass flux rates, the flame in the graded burner stabilizes further upstream, where the local Stanton number near the flame is higher, as compared to the step burner. The St values in Fig. 3b decrease with increasing mass flux, as illustrated in Fig. 1, although values for local St in the graded burner match those of the step burner at two to three times higher mass flux rates. The graded burner increases the heat exchange into the solid downstream of the flame, which, together with the smaller optical depth upstream, enhance interphase heat transfer and radiation feedback. This results in further preheating of the incoming reactants, thus delaying blow-off. The graded topology burner 1 (Fig. 2b) results in the maximum blow-off mass flux rate and reduced propensity for flashback, therefore this burner design was chosen for the experimental investigation.

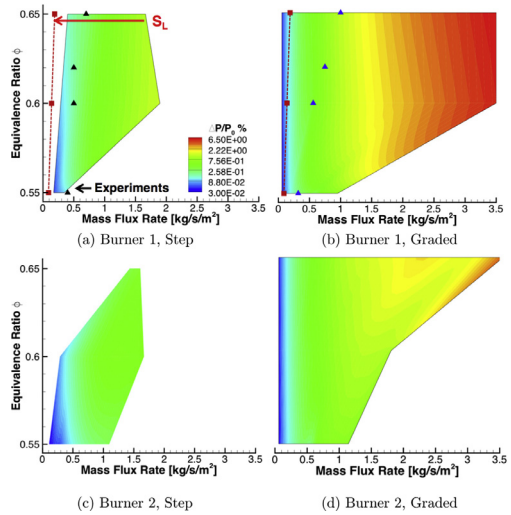

Fig. 2. Computational stability maps of (a,c) step and (b,d) graded topology burners 1 and 2, respectively, as well as mass flux rate associated with laminar flame speed indicated by S_L (dashed line) and experimental measurements (symbols).

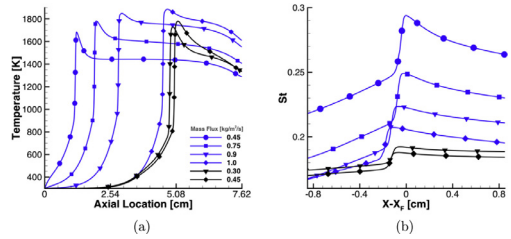

Fig. 3. (a) Gas temperature profiles at $\phi = 0.55$ corresponding to stability maps shown in Fig. 2a,b and (b) profiles centered at flame peak temperature location X_F for local St, for graded (blue) and step (black) profiles. (For interpretation of the references to color in this figure legend, the reader is referred to the web version of this article.)

3. Experimental investigation

3.1. Experimental setup and procedure

An experiment was designed to confirm computational results and examine the stability and

pressure drop characteristics of the graded burner in comparison to the step design. All experiments were performed using methane/air mixture at atmospheric pressure. Flow rates of reactants were measured and controlled using Alicat Scientific mass flow controllers. Compressed air and methane flows were mixed at a tee-junction approximately 200 tube diameters upstream of the burner to achieve a homogenous mixture prior to entry into the burner. The gauge pressure was measured immediately upstream of the burner using an Omega PX309 pressure transducer.

The burner consisted of different configurations of stacked ceramic foams that were wrapped in a layer of compressible ceramic insulation (Unifrax Fiberfrax 550-Grade Ceramic Fiber Paper) and housed in a quartz tube. The temperature was measured using K-type mineral-insulated thermocouples with standard limits (Watlow) placed between the porous media and the ceramic insulation. A thermocouple inserted inside a porous medium estimates the local solid temperature [19]. Zheng et al. [19] found that the difference between such thermocouple measurements and gas phase temperatures are < 25K, except near the reaction zone. As such, measured temperatures were used primarily for observing trends in flame location.

Hardware interfacing and data acquisition were performed using a National Instruments Data Acquisition system (NI-cDAQ 9188). All measured variables were logged automatically at 10Hz by a laboratory computer, and all controlled variables were specified using a LabVIEW interface. Maximum error in mass flux rate was $< 1\%$ and error in equivalence ratio was typically $< 3\%$, not exceeding 12% at the extinction limit. Thermocouple and pressure transducer errors were reported by the manufacturer as $\pm 0.75\%$ and $\pm 0.25\%$ of measured value, respectively. The system was ignited directly downstream of the porous media while supplied with lean premixed methane/air at a condition corresponding to the laminar flame speed. The first thermocouple was placed 1.3 cm upstream of the porous media to monitor for flashback, but this phenomenon was not observed in the current study and instead the flame eventually extinguished with decreasing mass flux rate. Six subsequent thermocouples were placed downstream at azimuthal locations varying by 90°. The locations of the thermocouples are shown by the symbols in Fig. 5b.

Stable operation was defined as continuous operation with no changes in thermocouple measurements greater than 5 K over 5 min. After reaching steady state, the stability limits were determined by changing the equivalence ratio (at a constant mass flux) to the condition under consideration, and subsequently increasing (or decreasing) the mass flux (at a constant equivalence ratio) in increments of $0.05\ kg/m^2s$. The blow-off limit was determined first by the occurrence of the maximum temperature measurement at the thermocouple furthest downstream, and subsequently by the continual decrease in temperature measured by this thermocouple. In the step PMB, blow-off was also confirmed visually by observing the gradual lift-off of the flame from the interface followed by lift-off from the downstream end of the porous media.

The SiC porous matrix was manufactured by LANIK. Ceramic porous materials are commonly manufactured based on pore density. To create an axially variable profile, the manufacturer used disks of polyurethane foams with increasing pore densities, each with a height of 1.27 cm and a diameter of 5.08 cm. Six disks, ranging from 65 to 10 ppi, were first dipped in a ceramic slurry, and while wet, glued in ascending order of pore density. Once dry, the disks were sintered together to create a continuous porous material with a height of 7.62 cm (see Fig. 4). The step burner was designed by stacking a 10 ppi and a 65 ppi SiC sample, each 3.81 cm in height, in the quartz tube. For both the step and graded burners, pore diameter increased in the direction of the flow but maintained a relatively constant porosity of approximately 75% and 78% in the graded and step PMB, respectively. The methodology for extracting pore topology profiles is discussed next.

3.2. Micro-CT and analysis of the porous foam

All samples that were experimentally investigated in the present work were analyzed using Micro-Computed Tomography (Micro-CT). Each sample was scanned using a GE eXplore CT 120 scanner with the following acquisition parameters: 25 μm resolution, 80 kVp tube energy, 32 mA current and 1200 projections over 360°. The reconstructed gray-scale images were first smoothed using a 2D bilateral filter, and then binarized using a 3D constant threshold. The porosity was extracted along the axial location of the sample as the ratio of gas voxels over the total number of voxels, averaged over each cross-sectional slice. The pore and cell diameters were identified by using a 3D distance transform watershed algorithm followed by a 3D particle analyzer [20,21]. Measurements of mean pore and cell diameters along each cross-flow slice for the step and graded porous matrices are shown in Fig. 4.

3.3. Results and discussion

The experimental results for flame stability, temperature, and pressure drop are shown in Fig. 5. The flame stability maps, in Fig. 5a, for both designs tested, qualitatively confirm a minimum 50% enhancement in flame stability, as found in the computational investigation. Thermocouple temperature measurements for both burners are shown in Fig. 5b, and compared to solid temperatures

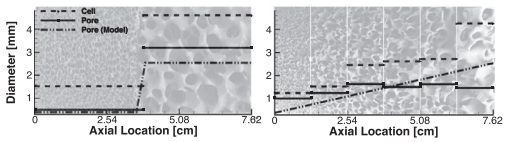

Fig. 4. Average pore and cell diameters for step (left) and graded (right) PMBs, as well as nominal pore diameters used in the model.

predicted by the model discussed in Section 2. Since the thermocouples are placed between the porous matrix and the surrounding ceramic insulation, measured temperatures are expected to be lower than those corresponding to the 1D volume-averaged simulation due to radial heat losses.

The pressure drop for mutually stable operating conditions is shown in Fig. 5c, where error bars represent variations in pressure drop depending on the location of flame stabilization for a given operating condition. As predicted, pressure drop is higher in the graded burner, but does not exceed 5.4% at the highest mass flux rate (2.34 kg/m^2s). Although both burners are made from the same material, and therefore have similar heat conduction properties, the solid temperatures are higher upstream of the flame in the graded PMB, due to the increased radiative heat transfer. Therefore, not only is the heat exchange between the gas and solid enhanced, as predicted by the Stanton number profile in Fig. 3b, but also the lower radiative extinction properties in the graded burner enables more effective heat recirculation. The consequence of the enhanced radiative heat feedback in the graded burner is increasingly relevant at higher equivalence ratios, where higher mass flux rates are supported. As illustrated in Fig. 1, the heat exchange between the solid and gas decreases as mass flux rates increase, which lowers preheat temperatures and eventually results in blow-off. In the experiment, dynamic stabilization of the flame was observed in the graded topology PMB, whereas the step topology PMB anchored the flame at the interface, as expected from the burner design and computational predictions.

Although the 1D model qualitatively captures trends in flame stability and pressure drop, deficiencies are apparent. This can be partially explained by the Micro-CT analysis of the porous foams, which revealed a deviation from the nominal pore diameter and an inconsistent trend in cell and pore diameter in some sections (see Fig. 4). Specifically, the presumed gradation in the pore diameter profile, based on the foam pore density, is less pronounced. However, there is a clear gradation in the cell diameter. As discussed in Section 2.1, existing closure models for 1D volume-averaged governing equations in porous media combustion are mainly parameterized by porosity and pore diameter, assuming these features are the only free parameters in the geometry. However, this does not account for independent variations in other topological features, such as cell diameter, as prescribed by the fabrication method. Additionally, to avoid specifying discontinuities in the numerical solution, the interface between differing topologies is either smoothed or represented as a continuous profile. Approximation of the related physical parameters and topology discontinuities may attribute to the discrepancy between the model predictions and experimental observations. Further model development is therefore needed to accurately capture the effects of pore-scale physics and structure in volume-averaged simulations.

4. Conclusions

Theoretical, computational and experimental investigations were conducted to explore the

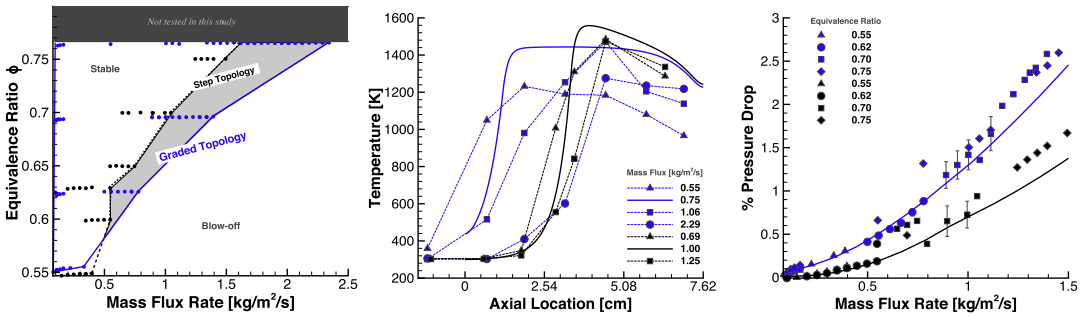

Fig. 5. (a) Experimental stability maps, (b) thermocouple measurements (symbols, dashed lines) at $\phi = 0.75$ compared to the model (solid lines), and (c) pressure drop measurements compared to the model for $\phi = 0.7$ (solid lines), for graded (blue) and step (black) profiles. (For interpretation of the references to color in this figure legend, the reader is referred to the web version of this article.)

performance benefits of topology grading in porous media combustion. Gradation was motivated by theoretically examining the governing equations and constitutive relations, revealing the significance of pore topology on interphase heat exchange and radiative heat transfer properties, and consequently on the flame stability. Specifically, the local Stanton number and optical depth were proposed as the quantities of interest for predicting trends in dynamic flame stabilization. Results from 1D simulations showed an extensive improvement in flame stability between step and graded topology burners, in particular for a graded pore diameter and constant porosity profile. This design was chosen for the experimental investigation of graded versus step topology PMBs, which qualitatively confirmed an enhancement of flame stability by $\sim 50\%$.

Although the 1D volume-averaged model in conjunction with empirical model coefficients qualitatively captures trends in flame stability for different porous matrix designs, the results do not quantitatively match those of the corresponding experiment. This motivates further development of volume-averaged models and macro-scale transport properties for application to burners with spatially variable pore topologies. Nonetheless, the investigation of matrix gradation in PMBs reveals the potential for tailoring the internal heat transfer properties to optimize performance. In addition to topology grading, which is presented as a means to modulate the radiative and interphase heat transfer modes, the thermal properties of the solid matrix itself can be functionalized by a composition gradient to further enhance burner performance. In this work, the graded porous matrix topology was experimentally investigated by considering a step-wise sequence of porous disks. However, recent progress in additive manufacturing techniques of ceramics such as preceramic polymers, powder-based laser sintering, and stereolithography [22] provide attractive opportunities for the construction of tailored pore topologies and materials for PMBs. Exploring this is the subject of future work.

Acknowledgments

This work is supported by a Leading Edge Aeronautics Research for NASA (LEARN) grant (No. NNX15AE42A) and by the National Science Foundation Graduate Research Fellowship (No. 1656518). We would also like to acknowledge LANIK for providing the porous materials.

References

[1] J. Howell, M. Hall, J. Ellzey, *Prog. Energy Combust. Sci.* 22 (2) (1996) 121–145.
[2] M.A. Mujeebu, M.Z. Abdullah, A. Mohamad, M.A. Bakar, *Prog. Energy Combust. Sci.* 36 (6) (2010) 627–650.
[3] J. Buckmaster, T. Takeno, *Combust. Sci. Tech.* 25 (3–4) (1981) 153–158.
[4] Y. Kotani, T. Takeno, *Proc. Combust. Inst.* 19 (1) (1982) 1503–1509.
[5] D. Trimis, F. Durst, *Combust. Sci. Tech.* 121 (1–6) (1996) 153–168.
[6] A.J. Barra, G. Diepvens, J.L. Ellzey, M.R. Henneke, *Combust. Flame* 134 (4) (2003) 369–379.
[7] S. Voss, M. Mendes, J. Pereira, S. Ray, J. Pereira, D. Trimis, *Proc. Combust. Inst.* 34 (2) (2013) 3335–3342.
[8] A. Bakry, A. Al-Salaymeh, A.H. Al-Muhtaseb, A. Abu-Jrai, D. Trimis, *Fuel* 90 (2) (2011) 647–658.
[9] S. Mullens, J. Luyten, J. Zeschky, Characterization of Structure and Morphology, in: Cellular Ceramics, Wiley-VCH Verlag GmbH & Co. KGaA, pp. 225–266.
[10] A.P. Philipse, H.L. Schram, *J. Am. Ceram. Soc.* 74 (4) (1991) 728–732.
[11] S. Sobhani, B. Haley, D. Bartz, J. Dunnmon, J. Sullivan, M. Ihme, in: ASME Turbo Expo 2017: Turbomachinery Technical Conference and Exposition, 50893, 2017, doi:10.1115/GT2017-63204. V05CT17A001.
[12] J. Howell, M. Menguc, R. Siegel, *Thermal Radiation Heat Transfer, 5th Edition*, Taylor & Francis, 2010.
[13] P.-F. Hsu, J.R. Howell, *Exp. Heat Transf.* 5 (4) (1992) 293–313.
[14] V.M. Patel, P. Talukdar, *Int. J. Therm. Sci.* 108 (2016) 89–99.
[15] C. Bedoya, I. Dinkov, P. Habisreuther, N. Zarzalis, H. Bockhorn, P. Parthasarathy, *Combust. Flame* 162 (10) (2015) 3740–3754.
[16] D.G. Goodwin, H.K. Moffat, R.L. Speth, 2017, (http://www.cantera.org). Version 2.3.0.
[17] C.T. Bowman, R.K. Hanson, D.F. Davidson, et al. GRI-Mech 2.11, 1995, Available from http://www.me.berkeley.edu/gri-mech/.
[18] J.C. Ferguson, F. Panerai, A. Borner, N.N. Mansour, *SoftwareX* 7 (2018) 81–87.
[19] C. Zheng, L. Cheng, A. Saveliev, Z. Luo, K. Cen, *Proc. Combust. Inst.* 33 (2) (2011) 3301–3308.
[20] D. Legland, I. Arganda-Carreras, P. Andrey, *Bioinformatics* 32 (22) (2016) 3532–3534.
[21] E. Maire, P. Colombo, J. Adrien, L. Babout, L. Biasetto, *J Eur. Ceram. Soc.* 27 (4) (2007) 1973–1981.
[22] Z.C. Eckel, C. Zhou, J.H. Martin, A.J. Jacobsen, W.B. Carter, T.A. Schaedler, *Science* 351 (6268) (2016) 58–62.